Characterization of Periodic and Aperiodic Activity of Single-Channel in-Ear Electroencephalography

Camille Rakotoranto and Alejandro López Valdés, *Senior Member IEEE*

***Abstract*— Ear-electroencephalography (ear-EEG) is a discreet, wearable EEG alternative suitable for ambulatory and long-term monitoring, especially with rising demand for smart wearables and increasing neurological disorders. Its wider adoption has been limited by reduced signal quality. The Fitting Oscillations and One-Over-f (FOOOF) algorithm, used in scalp-EEG to separate periodic brain rhythms from the non-oscillatory aperiodic component, may improve interpretability. This study presents the first application of FOOOF to ear-EEG, assessing its ability to produce reliable, scalp-equivalent neural metrics. Synchronous scalp and ear-EEG were recorded during resting state and alpha block paradigms. A calibrated FOOOF pipeline extracted periodic and aperiodic activity. Results showed that FOOOF improved comparability between modalities, particularly between ear and inter-hemispheric scalp configurations. Periodic metrics showed strong agreement, with correlations up to 0.90 between FOOOF-adjusted peak alpha power in ear- and scalp-EEG. The aperiodic exponent showed no significant differences between them. These findings indicate that single-channel ear-EEG, when processed with FOOOF, can deliver accurate neural metrics comparable to scalp-EEG. This positions ear-EEG as a promising tool for outpatient neuro-monitoring, with potential applications in epilepsy, cognitive decline, and sleep disorder assessment.**

***Clinical Relevance*— FOOOF-adjusted ear-EEG could enhance ambulatory, non-intrusive wearable technology, with applications in neurodegenerative disease diagnosis, monitoring, and wellness.**

I. Introduction

Conventional scalp-electroencephalography (EEG) offers high temporal resolution but remains bulky and impractical for continuous, real-world health monitoring [1, 2]. Ear-EEG – using electrodes placed in or around the ear – is a promising wearable alternative but suffers from weakened signals, including lower amplitudes and signal-to-noise ratios (SNR) [3-5]. Nevertheless, dry electrode ear-EEG systems, such as the IDUN earbuds, can capture neurologically relevant oscillations like alpha rhythms during the resting state (RS) and alpha block [6]. More generally, Looney et al. demonstrated that ear-EEG can reliably detect significant alpha desynchronizations, such as the expected reduction in alpha power following eye opening, despite its inherently weaker signal characteristics [1].

Recent EEG signal analysis has emphasized the importance of distinguishing between periodic and aperiodic components of the power spectral density (PSD), the latter exhibiting 1/f-like behavior [7, 8]. Periodic activity reflects synchronized neural oscillations linked to cognitive and behavioral states, whereas aperiodic features provide insight into background neural activity, cortical excitability, and neurodevelopmental conditions. The Fitting Oscillations and One-Over-f (FOOOF) algorithm models these components separately, improving both interpretability and diagnostic utility [7].

Traditional EEG analysis often conflates periodic components, leading to ambiguous results [9]. FOOOF iteratively models the EEG PSD by fitting Gaussian functions to oscillatory peaks while simultaneously modeling the aperiodic activity using power-law fitting. This effectively separates these components to extract metrics such as peak frequencies, bandwidth, and power, alongside aperiodic parameters (exponent and offset). While most decomposition techniques isolate oscillatory activity, only FOOOF explicitly models the aperiodic background, yielding more reliable, specific, and interpretable neural markers. As demonstrated across the literature [7-12], FOOOF-derived features have been successfully applied in a range of clinical contexts. These include outpatient applications such as anesthesia depth monitoring via more accurate delta wave tracking and cognitive fatigue assessment [8], as well as neurological disorders like age-related neural decline [8-10], schizophrenia [11], and epilepsy [12]. Together, these applications have demonstrated distinct improvements over conventional approaches in enhancing patient outcomes. However, FOOOF has yet to be applied to ear-EEG, limiting its use in wearable, ambulatory monitoring contexts.

Given the inherent limitations of ear-EEG and the challenges in realizing FOOOF's potential, this study explores their synergy by presenting the first systematic application of FOOOF to single-channel ear-EEG. The study validates its compatibility, comparing FOOOF-derived metrics between the ear and scalp, and evaluating signal quality to identify scalp configurations most correlated with ear-EEG. This work lays the groundwork for a viable solution for continuous brain monitoring beyond laboratory settings.

II. Methods

A. Participants

Sixteen healthy adults (mean age = 22.5 ± 2.2 years; 5 males, 11 females) participated, with eight datasets obtained from a previous ear-EEG validation study using an identical methodology to ensure consistency [13]. Participants without

C. Rakotoranto is with the School of Engineering, Trinity College Dublin, The University of Dublin, Ireland (e-mail: rakotorc@tcd.ie).

A. Lopez Valdes is with the School of Engineering, Trinity College Dublin, The University of Dublin, Ireland; Trinity Centre for Biomedical Engineering, Ireland; Trinity College Institute for Neuroscience, Ireland; and the Global Brain Health Institute, Ireland (e-mail: alejandro.lopez@tcd.ie).

neurological disorders or implants were selected to minimize confounding factors [13]. Both sexes were included based on recruitment availability. Ethical approval was granted by the Trinity College Dublin Research Ethics Committee (Ref: 3831), and participants provided informed consent.

B. Data Collection

Brain activity was recorded synchronously using ear- and scalp-EEG. For ear-EEG, single-channel IDUN Guardian Earbuds (IDUN Technologies AG) were utilized, with the right ear referenced to the left ear electrode. Participants inserted the sanitized earbuds, which were then adjusted for fit and to maintain impedance below 300 kΩ. Wireless data streaming was performed at 250 Hz using Python SDK. A 24-channel scalp-EEG cap (Easycap GmbH, Germany) was used as the reference for characterization. Cap sizes were adjusted for individual anatomy, with impedance maintained below 20 kΩ using conductive gel. mBrainTrain Mobi amplifier (mBrainTrain LLC, Belgrade) was used to collect data at 250 Hz, with wireless transmission via a BlueSoleil v10 USB dongle. Paradigms were implemented using the validated EaR-P Lab application, with temporal synchronization ensured via LabStreaming Layer (LSL, Swartz Centre for Computational Neuroscience, UC San Diego, USA) across the Python SDK, mBrainTrain, and EaR-P Lab data streams [14]. All applications were run on a Dell laptop positioned 60 cm from participants at eye level, with auditory stimuli delivered using HD 280 Pro headphones (Sennheiser, Germany) at 10% volume in a non-shielded behavioral testing room.

EEG paradigms consisted of a five-minute resting state (RS) recording and a four-minute Alpha Block task with one-minute alternating eyes open (EO) and eyes closed (EC). Data recordings proceeded without issues, allowing all datasets to be retained for analyses. However, the raw RS EEG file for Participant 3 and the Alpha Block EEG file for Participant 8 from the previous study were unreadable, likely due to file corruption, and were excluded.

C. Pre-Processing and FOOOF Application

Raw EEG data from the RS and Alpha Block paradigms were pre-processed using custom MATLAB scripts (MATLAB R2024b, The MathWorks Inc., Natick, MA, USA). All scripts are publicly available on GitHub (https://github.com/rakotc/Parameterization-of-Ear-EEG). The Alpha Block data was separated into EC and EO segments using synchronized markers, resulting in three conditions overall: RS, EC, and EO. Both modalities' signals were band-pass filtered (1 to 100 Hz) to remove artifacts and drifts, with a 50 Hz notch filter applied to reduce powerline noise. Independent Component Analysis (ICA) was not used due to the single-channel nature of ear-EEG and to ensure unbiased comparison across modalities. Scalp-EEG was referenced into three configurations (T7-Oz, T8-Oz, T7-T8). PSDs were calculated using Welch's method with 2 s windows and 50% overlap.

FOOOF parameters were tuned on a subset of data from different subjects across RS, EC, and EO conditions using the T7-Oz and T8-Oz configurations. An iterative MATLAB script optimized parameters based on goodness-of-fit metrics to avoid under- and overfitting. The final parameters (maximum peaks = 11, minimum peak height = 0.05, peak threshold ratio = 1.5 and peak width limits = [1.1, 7] Hz) achieved a strong quality fit (mean R^2 = 0.97), and the parameters generalized well to other configurations, including ear-EEG where the highest fit correlation was obtained (R^2 = 0.985, Fig. 1 (A) and (B)).

FOOOF was applied to data in the 2 to 100 Hz range, and fixed or knee aperiodic models were selected based on the best quantitative fit quality. The algorithm extracted periodic parameters (peak power, frequency, bandwidth) and aperiodic parameters (exponent, offset), along with fit metrics. The alpha band (8 to 12 Hz) peak power and SNR in decibels, calculated via equation (1), were used to analyze oscillatory activity for all conditions and configurations. Similarly, the aperiodic exponent was used to characterize background neural activity.

$$SNR = Average\ Alpha\ Power_{EC} - Average\ Alpha\ Power_{EO} \quad (1)$$

D. Statistical Analyses

The statistical analyses addressed the study's three primary aims and were carried out using custom MATLAB scripts and

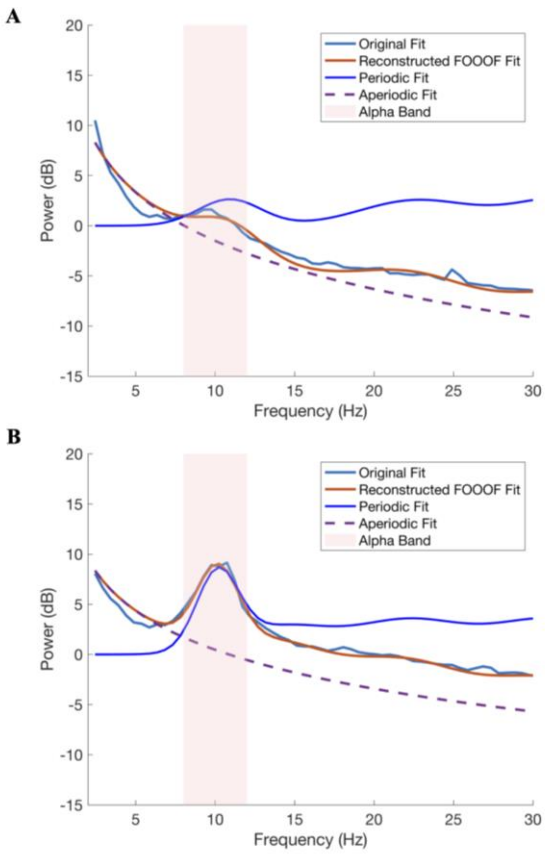

Fig. 1. Decomposition of EC average PSD into periodic and aperiodic fits using FOOOF, for different configurations: **(A)** Ear, and **(B)** T7-Oz (n = 15).

Prism 10 (GraphPad Software, Boston, USA). Outliers were identified using a ROUT test (Q = 1%), and normality was assessed using the Shapiro-Wilk test. G*Power was used to examine non-significant results for statistical power further.

To validate the cohort datasets, inter-gender comparisons of pre-and post-FOOOF peak alpha power and SNR, as well as aperiodic exponent, were conducted across all conditions and configurations using unpaired t-tests or Wilcoxon rank-sum tests, depending on data distribution. Validation of FOOOF's performance involved comparing pre- and post-FOOOF peak alpha power and SNR values within each configuration (Ear, T7-Oz, T8-Oz, T7-T8) across the RS, EC, and EO conditions, using paired t-tests or Wilcoxon signed-rank tests.

Inter-configuration comparisons were made to evaluate ear-EEG relative to scalp-EEG by comparing peak alpha power, SNR, and aperiodic exponent values across conditions, again using the appropriate statistical tests. Correlations between ear and scalp configurations were assessed using Spearman correlation, utilized for its robustness to non-normal data distributions. To assess hemispheric balance and the representativeness of inter-hemispheric configurations, comparisons were made between T7-Oz and T8-Oz for peak alpha power, SNR, and aperiodic exponent. Following this, a gold-standard average of the T7-Oz and T8-Oz metrics was computed and compared to the T7-T8 and ear-EEG configurations to evaluate their signal quality. All analyses followed consistent procedures to ensure comparability and reliability across metrics and conditions.

III. Results

A. Validation of FOOOF for Ear-EEG

Given the absence of significant differences in periodic and aperiodic activities between genders ($p > 0.05$), the full dataset was utilized for characterization. Post-hoc power calculations indicated values above 0.85 for all comparisons, confirming sufficient sensitivity to detect effects within the cohort. Subsequently, scalp configurations consistently exhibited reductions in peak alpha power across all conditions. For example, T7-Oz demonstrated a 24% decrease in RS and a significant reduction in EC ($p < 0.001$). In contrast, ear-EEG showed a consistent but nonsignificant increase in peak alpha power, including a 1.42-fold rise in RS and up to a 2.79-fold in the EO condition.

Nonetheless, all configurations demonstrated a reduction in the SNR post-FOOOF, with this drop being significant for all scalp configurations ($p < 0.01$), but not for ear-EEG ($p > 0.05$).

B. Inter-Configuration Comparisons

As illustrated in Fig. 2 (A) – (F), FOOOF adjustment reduced the magnitude of differences in peak alpha power between modalities across all conditions. Importantly, the largest reduction was 59% in the EO condition between the ear and T7-Oz. For EC, the ear's peak alpha power remained significantly lower than hemispheric scalp configurations ($p < 0.05$), but not compared to T7-T8 ($p > 0.05$). In contrast, as shown in Fig. 2 (A) and (B), discrepancies in RS between the

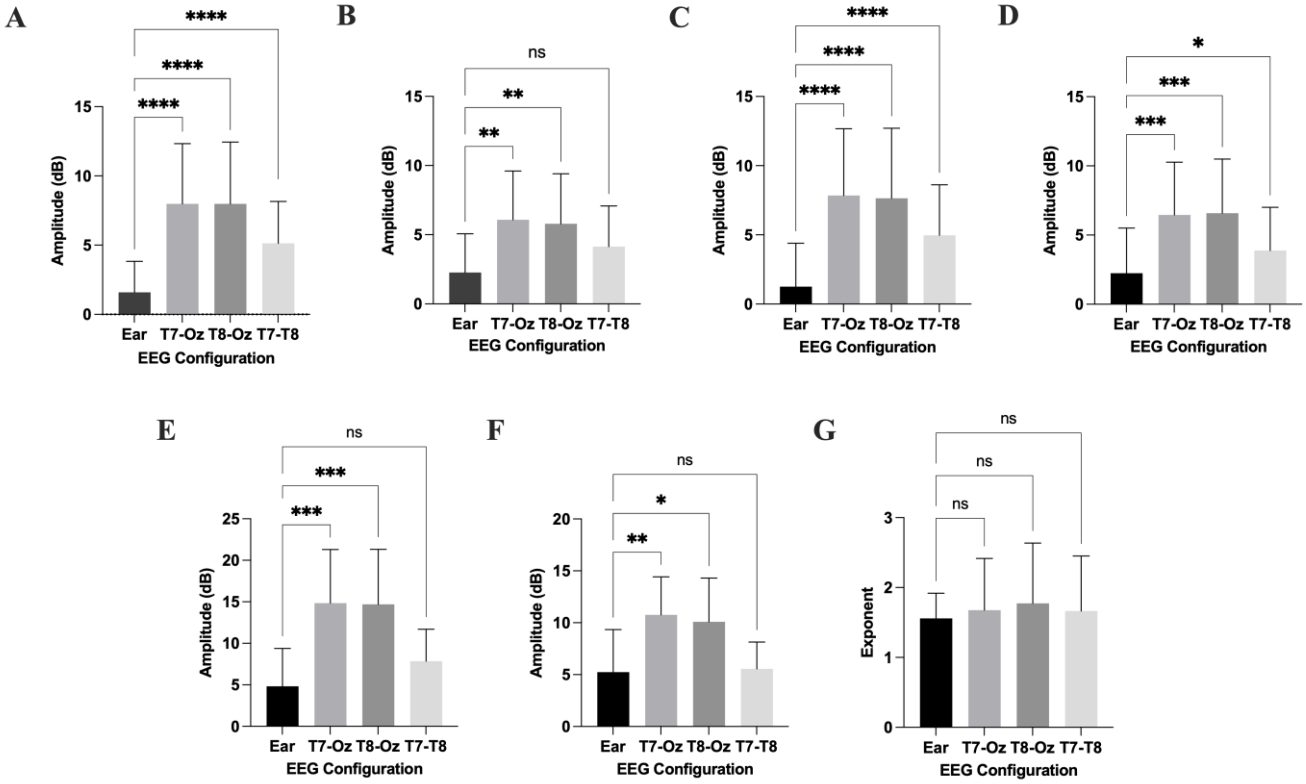

Fig. 2. Comparison of ear-EEG and scalp-EEG configurations before and after FOOOF adjustment across various conditions. **(A)** Peak alpha power in RS - Pre-FOOOF, **(B)** FOOOF-adjusted periodic fit; **(C)** Peak alpha power in EO - Pre-FOOOF, **(D)** FOOOF-adjusted periodic fit; **(E)** Peak alpha power in EC - Pre-FOOOF, **(F)** FOOOF-adjusted periodic fit; and **(G)** Comparison of RS aperiodic exponents. Statistical significance was assessed using paired t-tests. Values are presented as mean ± SD (n = 15). *$p < 0.05$, **$p < 0.01$, ***$p < 0.001$, ****$p < 0.0001$.

ear and T7-T8 reduced from highly significant ($p < 0.0001$) to nonsignificant ($p > 0.05$) post-FOOOF.

Correlation analyses summarized in Table 1 confirmed that T7–T8 exhibited the strongest positive correlation with ear-EEG in peak alpha power, with a post-FOOOF coefficient of 0.90 during EO. Regarding the aperiodic exponent, no consistent configuration correlated best with the ear. Although the ear showed the lowest exponent in the RS condition (1.56 ± 0.36), no significant differences were observed between the ear and scalp configurations across any condition ($p > 0.05$). Generally, Fig. 2 (G) illustrates the RS results as representative of this broader pattern across all conditions. Moreover, post-hoc power calculations exceeded 0.92 for all conditions, supporting the adequacy of detecting these effects using this sample size.

Further analysis of Table 1 revealed that, while the ear originally exhibited comparable correlations with T7-Oz and T8-Oz, some deviations emerged in the RS condition following FOOOF adjustment, in both peak alpha power and aperiodic exponents. In line with this variability, eye closure demonstrated improved correlations post-FOOOF, whereas no clear pattern was observed for the RS and EO conditions.

C. Quality Evaluation Against Hemispheric Gold Standard

To establish a gold standard, parameters from T7-Oz and T8-Oz were compared. No significant differences in FOOOF-adjusted peak alpha power, SNR, or aperiodic exponent were found between the two hemispheric configurations across all conditions. Therefore, their average was used as the reference standard for evaluating the quality of the ear and T7-T8 inter-hemispheric configurations.

Post-FOOOF, both configurations exhibited varying reductions in statistical significance relative to the reference. For instance, in some conditions (e.g., RS), the T7-T8 configuration became nonsignificant, while in others (e.g., EC,

TABLE 1. CORRELATION BETWEEN EAR AND SCALP CONFIGURATIONS ACROSS CONDITIONS. COLOR SCALE RANGES FROM NEGATIVE CORRELATION (RED) TO POSITIVE CORRELATION (GREEN).

		Parameter	Paradigm	T7-Oz	T8-Oz	T7-T8
Pre-FOOOF		***Peak Alpha Power***	***Resting State***	0.34	0.34	0.61
			Eyes Closed	0.14	0.25	0.39
			Eyes Open	0.79	0.78	0.84
FOOOF-Adjusted	***Periodic***	***Peak Alpha Power***	***Resting State***	- 0.04	0.30	0.51
			Eyes Closed	0.71	0.66	0.74
			Eyes Open	0.68	0.61	0.90
	Aperiodic	***Exponent***	***Resting State***	0.37	0.00	0.14
			Eyes Closed	- 0.04	- 0.50	- 0.03
			Eyes Open	- 0.30	- 0.64	- 0.11

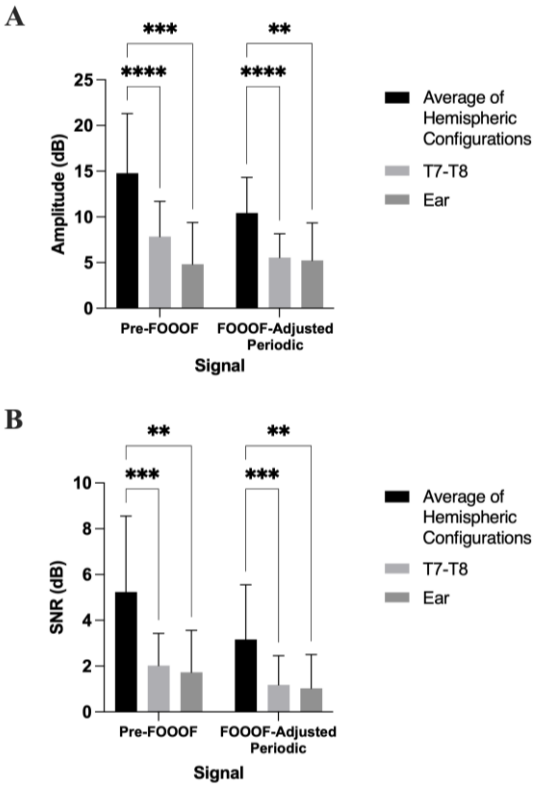

Fig. 3. Comparison of ear and scalp inter-hemispheric configurations against the average scalp hemispheric gold standard. **(A)** EC peak alpha power and **(B)** SNR. Values are presented as mean ± SD (n = 15). $^{**}p < 0.01$, $^{***}p < 0.001$, $^{****}p < 0.0001$.

Fig. 3 (A)), significant differences remained (ear: $p < 0.01$, T7-T8: $p < 0.0001$). Similarly, no consistent SNR trend emerged across conditions, but ear-EEG remained more comparable to the gold reference post-FOOOF, as seen in Fig. 3 (B) ($p < 0.01$). A statistical power calculation exceeding 0.90 further supported the reliability of these findings.

IV. DISCUSSION

Dataset validation confirmed the absence of significant gender-based differences in periodic and aperiodic components within the narrow, healthy demographic and aligned with known trends in alpha power, thus supporting the robustness of the cohort [9, 15]. Applying FOOOF to scalp-EEG performed as expected, reducing periodic activity due to the removal of 1/f aperiodic noise. In contrast, ear-EEG showed nonsignificant increases in peak alpha power post-FOOOF. This may be due to the absence of artifact rejection, which can leave residual non-neural noise, such as muscle and motion artifacts, unaddressed. In noisy modalities like ear-EEG, narrowband transient artifacts may not be captured by the aperiodic fit, causing them to be misclassified as periodic peaks. Consequently, residual noise can inflate peak power estimates, diminishing the effectiveness of the FOOOF decomposition. Nonetheless, artifact rejection was deliberately excluded to avoid bias, particularly because standard methods, such as ICA, are incompatible with single-channel ear-EEG, and alternative techniques lack validation or impose a significant computational load [7].

Despite a persistent lower absolute peak alpha power, ear-EEG became more comparable to scalp recordings following FOOOF adjustment. The strongest correspondence was observed with the inter-hemispheric configuration T7–T8, which showed correlation coefficients of up to 0.90 and improvements in both EC and EO conditions (Fig. 2 (A) – (F)). This reflects the anatomical proximity between the ear and the latter, which results in the detection of more comparable volume-conducted signals. Thus, while all configurations measure the same neural sources, the characteristics of these periodic signals are strongly influenced by spatial sampling as explored in the literature [2, 9]. Contrarily, aperiodic parameters remained consistent across all sites, reinforcing the spatial invariance and robustness of the aperiodic exponent – even in noisier, single-channel ear-EEG such as those analyzed without artifact rejection. This spatial invariance arises from the global nature of aperiodic activity, which reflects large-scale cortical dynamics and the brain-wide balance between excitatory and inhibitory processes; these features are less dependent on the signal sources [7, 9, 11].

Most importantly, signal quality assessment addressed a key gap in the literature. Although FOOOF did not consistently improve signal quality in either modality compared to the gold reference, both ear-EEG and inter-hemispheric scalp configurations showed no clear advantage over each other, demonstrating similar variability in spectral fidelity relative to the reference while maintaining comparability between themselves. Separating periodic and aperiodic components is particularly crucial for ear-EEG, where the inherently lower signal amplitudes and higher susceptibility to noise and motion artifacts traditionally make it difficult to distinguish genuine neural activity from broadband distortions. However, FOOOF's explicit modeling and isolation of both periodic and aperiodic activity in ear-EEG – unlike conventional decomposition algorithms – mitigated these issues, improving interpretability and minimizing differences between ear- and scalp-EEG. These findings represent a significant advancement toward more user-friendly, effective, and personalized treatment of neurological disorders – including dementia [9, 10, 16, 17], schizophrenia [11], and epilepsy [16, 17] – as well as sleep disorders [16-18]. This progress is driven by the reliable decomposition of ear-EEG PSDs. While prior studies have demonstrated the feasibility of ear-EEG-based monitoring for these conditions, challenges with signal quality compared to scalp-EEG have limited diagnostic accuracy – a limitation that this novel combined approach can effectively overcome.

Nonetheless, these findings should be interpreted in light of the inter-subject variability observed in ear-EEG, likely stemming from anatomical differences and the inevitable constraints of generic-fitting earbuds [3, 6]. This variability contributed to a larger SNR variation reflected by a greater standard deviation, highlighting the need for artifact rejection and improved device ergonomics to ensure reliable real-world use. It may also account for the lower correlations observed post-FOOOF in Table 1, despite the absence of significant differences in the corresponding measures (Fig. 2 (G)). Furthermore, the restricted demographic may have limited neural variability, as gender- and age-related EEG differences typically emerge later in life due to cumulative neurostructural and hormonal changes [9]. Thus, while post-hoc power analyses and effect sizes indicated sufficient sensitivity, the statistical generalizability of these findings must be validated in future studies employing larger and more diverse cohorts. Given the projected use of FOOOF-adjusted ear-EEG for outpatient and long-term monitoring in real-world settings, addressing these limitations is critical to ensure reliable and robust performance across various populations and conditions.

While this study establishes the foundational comparability of ear-EEG to gold standard configurations, its practical deployment for mobile brain monitoring demands further investigation. This begins with the identification of compatible artifact rejection methods; Noise-Assisted Multivariate Empirical Mode Decomposition has been proposed, but its validity and computational feasibility remain underexplored [19]. Alternatively, the FOOOF algorithm itself could be adapted to better handle the distinct noise characteristics of ear-EEG. For instance, condition-specific frequency fitting windows could exclude artifact-dominant bands, and penalty-informed fitting – which suppresses abnormally located peaks and steep slopes using regularization, could improve robustness. These modifications may address the non-oscillatory-like behavior observed within the FOOOF-adjusted periodic fit beyond 15 Hz (Fig. 1), as well as the inconsistent correlation patterns between ear and scalp configurations across conditions (Table 1), both of which likely reflect the residual artifacts in the current FOOOF-adjusted fits.

Beyond these algorithmic improvements, FOOOF-adjusted ear-EEG must be validated under ecologically valid conditions involving longer durations and participant movement to evaluate its performance in realistic settings. Moreover, while FOOOF-adjusted ear-EEG shows promise for ambulatory monitoring, its current implementation – requiring the complete signal – restricts its use in live applications. Considering the surge in wearable technologies, future work should explore whether FOOOF can be implemented in real-time, such as through an overlapping-window PSD estimation and gradual update of parameters. This development would extend this technology's utility beyond neurological diagnostics to broader applications in health and wellness, leveraging EEG's ability to capture systemic physiological states [9].

Taken together, the statistical equivalence between ear-EEG and the clinically accepted T7–T8 configuration addresses the critical issue of inferior signal quality that has traditionally limited ear-EEG's use in continuous brain monitoring for conditions such as schizophrenia [11], cognitive decline [9-11, 16, 17], and sleep disorders [16-18]. Nonetheless, further refinement is required to match the robustness of more spatially optimal established clinical configurations, such as T7-Oz and T8-Oz, alongside improvements in artifact handling, device design, and remote testing to ensure reliable practical deployment.

V. Conclusion

This study presents the first characterization of ear-EEG's periodic and aperiodic components using FOOOF, addressing a critical gap in mobile brain monitoring. By minimizing discrepancies in periodic power between both modalities and confirming the spatial invariance of aperiodic activity,

FOOOF enhanced comparability between ear- and scalp-EEG. Notably, FOOOF-adjusted ear-EEG achieved signal quality comparable to a scalp montage, despite limitations. These findings pave the way for validating ear-EEG as a user-friendly alternative for continuous neurological health monitoring, with potential applications extending beyond clinical diagnostics and treatment to general health and wellness tracking. As algorithmic and ergonomic advances progress, FOOOF-adjusted ear-EEG is well-positioned to become a practical and scalable technology for real-world ambulatory health assessment.

REFERENCES

[1] D. Looney et al., "The In-the-Ear Recording Concept: User-Centered and Wearable Brain Monitoring," *IEEE Pulse*, vol. 3, no. 6, pp. 32–42, 2012.

[2] N. Kaongoen et al., "The future of wearable EEG: A review of ear-EEG technology and its applications," *Journal of Neural Engineering*, vol. 20, no. 5, 2023.

[3] J. Pazuelo et al., "Evaluating the Electroencephalographic Signal Quality of an In-Ear Wearable Device," *Sensors*, vol. 24, no. 12, p. 3973, 2024.

[4] K. B. Mikkelsen et al., "EEG recorded from the ear: characterizing the ear-EEG method," *Frontiers in Neuroscience*, vol. 9, p. 438, 2015.

[5] P. Kidmose et al., "Ear-EEG from generic earpieces: a feasibility study," in *Proc. 35th Annual International Conference of the IEEE Engineering in Medicine and Biology Society (EMBC)*, 2013, pp. 543–546.

[6] IDUN Technologies AG, "Validation of in-ear EEG for Sleep and Hearing Use Cases," IDUN Technologies AG, 2023.

[7] T. Donoghue et al., "Parameterizing neural power spectra into periodic and aperiodic components," *Nature Neuroscience*, vol. 23, no. 12, pp. 1655–1665, 2020.

[8] N. Brake et al., "A neurophysiological basis for aperiodic EEG and the background spectral trend," *Nature Communications*, vol. 15, no. 1, p. 1514, 2024.

[9] G. Ouyang et al., "Decomposing alpha and 1/f brain activities reveals their differential associations with cognitive processing speed," *NeuroImage*, vol. 205, p. 116304, 2020.

[10] A. M. Van Nifterick et al., "Resting-state oscillations reveal disturbed excitation–inhibition ratio in Alzheimer's disease patients," *Scientific Reports*, vol. 13, no. 1, p. 7419, 2023.

[11] E. J. Peterson et al., "Aperiodic Neural Activity is a Better Predictor of Schizophrenia than Neural Oscillations," *Clinical EEG and Neuroscience*, vol. 54, no. 4, pp. 434–445, 2023.

[12] N. Wagh et al., "Population-based spectral characteristics of normal interictal scalp EEG inform diagnosis and treatment planning in focal epilepsy," *Scientific Reports*, vol. 15, no. 1, p. 25147, 2025.

[13] J. K. Bradshaw Bernacchi and A. López Valdés, "Electrophysiological Characterisation of Commercial Ear-EEG Devices," in *Proc. 47th Annual International Conference of the IEEE Engineering in Medicine and Biology Society (EMBC)*, 2025.

[14] G. Correia, M. J. Crosse, and A. López Valdés, "Brain wearables: validation toolkit for ear-level EEG sensors," *Sensors*, vol. 24, no. 4, p. 1226, 2024.

[15] J.-H. Kang, J.-H. Bae, and Y.-J. Jeon, "Age-related characteristics of resting-state electroencephalographic signals and the corresponding analytic approaches: a review," *Bioengineering*, vol. 11, no. 5, p. 418, 2024.

[16] A. S. Mihai et al., "The Next Frontier in Brain Monitoring: A Comprehensive Look at In-Ear EEG Electrodes and Their Applications," *Sensors*, vol. 25, no. 11, p. 3321, 2025.

[17] J. Y. Juez et al., "Ear-EEG devices for the assessment of brain activity: a review," *IEEE Sensors*, vol. 24, no. 20, pp. 31606–31623, 2024.

[18] T. Nakamura et al., "Hearables: Automatic overnight sleep monitoring with standardized in-ear EEG sensor," *IEEE Transactions on Biomedical Engineering*, vol. 67, no. 1, pp. 203–212, 2019.

[19] Y. Liu et al., "Remove motion artifacts from scalp single channel EEG based on noise assisted least square multivariate empirical mode decomposition," in *Proc. 13th International Congress on Image and Signal Processing, BioMedical Engineering and Informatics (CISP-BMEI), BioMedical Eng. Informatics (CISP-BMEI)*, 2020.